

Anderson localization versus charge-density-wave formation in disordered electron systems

S. Nishimoto,¹ S. Ejima,² and H. Fehske²

¹Institute for Theoretical Solid State Physics, IFW Dresden, 01171 Dresden, Germany

²Institute of Physics, Ernst Moritz Arndt University Greifswald, 17489 Greifswald, Germany

(Received 3 August 2012; revised manuscript received 10 January 2013; published 18 January 2013)

We study the interplay of disorder and interaction effects including bosonic degrees of freedom in the framework of a generic one-dimensional transport model: the Anderson-Edwards model. Using the density-matrix-renormalization group technique, we extract the localization length and the renormalization of the Tomonaga-Luttinger-liquid parameter from the charge-structure factor by a elaborate sample-average finite-size scaling procedure. The properties of the Anderson localized state can be described in terms of scaling relations of the metallic phase without disorder. We analyze how disorder competes with the charge-density-wave correlations triggered by the bosons and give evidence that disorder will destroy the long-range charge-ordered state.

DOI: 10.1103/PhysRevB.87.045116

PACS number(s): 71.23.An, 71.27.+a, 71.30.+h, 71.45.Lr

I. INTRODUCTION

Disorder is an inherent part of any solid-state system.¹ Low-dimensional materials are exceedingly susceptible to disorder. In one dimension (1D), theory predicts that all carriers are strongly localized for arbitrary energies and arbitrarily weak disorder. This holds for Anderson's noninteracting tight-binding Hamiltonian with a diagonal (i.e., on-site) random potential.^{2,3} The coherent backscattering from the randomly distributed impurities thereby transforms the metal into an insulator.

In 1D, the mutual interaction of the particles is likewise of significance; here even weak interactions can cause strong correlations. The instantaneous Coulomb repulsion between the electrons, for instance, tends to immobilize the charge carriers as well. As a consequence, at half filling, a Mott insulating (spin-density-wave) phase is energetically favored over the metallic state.⁴ The retarded electron-phonon coupling, on the other hand, may lead to structural distortions accompanied by polaron formation,⁵ and is the driving force behind the metal-to-Peierls transition, establishing a charge-density-wave (CDW) order.⁶

An understanding of how disorder and interaction act together is of vital importance not only to discuss the metal-insulator itself but also to analyze the electronic properties of many quasi-1D materials of current interest, such as conjugated polymers, organic charge-transfer salts, ferroelectric perovskites, halogen-bridged transition-metal complexes, TMT[SF,TF] chains, Qn(TCNQ)₂ compounds, or, e.g., the quite recently studied vanadium dioxide Peierls-Mott insulator.^{7–10} Carbon nanotubes¹¹ and organic semiconductors¹² are other examples where disorder and bosonic degrees of freedom are of importance. Regarding interacting bosons, ultracold atoms trapped in optical lattices offer the unique possibility to tune both the disorder and interaction strength.¹³

Unfortunately, the subtle interplay of disorder and interaction effects is one of the most challenging problems in solid-state theory and—despite 50 years of intense research—is still an area of uncertainty; see Ref. 14 and references therein. In the limit of vanishing charge-carrier density, only the interaction with the lattice vibrations matters. Then Anderson disorder may affect the polaron self-trapping in

a highly nontrivial way.¹⁵ This has been demonstrated for the Anderson-Holstein model within the statistical dynamical mean-field and momentum-average approximations.^{16,17} At finite carrier density, the Mott-Anderson transition for Coulomb correlated electrons was investigated by self-consistent mean-field theory in $D = \infty$ and $D = 3$,^{18–20} as well as by variational Gutzwiller-ansatz-based approaches.²¹ Electron-electron interactions may screen the disorder potential in strongly correlated systems, thereby stabilizing metallicity.²² Exact results are rare, however. In 2D, Lanczos and quantum Monte Carlo data suggest a disorder-induced stabilization of the pseudogap, also away from half filling.²³ The density-matrix-renormalization group (DMRG)²⁴ allows the numerical exact calculation of ground-state properties of disordered, interacting fermion systems in 1D, on fairly large systems. Exploiting this technique, the properties of disordered Luttinger liquids have been analyzed in the framework of the spinless fermion Anderson-*t*-*V* model (At VM)²⁵ and the spinful Anderson-Hubbard model.²⁶

In this paper, we address how many-body Anderson localization competes with CDW formation triggered by bosonic degrees of freedom in the framework of the Anderson-Edwards model (AEM).

II. MODEL

The Edwards model²⁷ represents a very general two-channel fermion-boson Hamiltonian, describing quantum transport in a background medium. Its fermion-boson interaction part

$$H_{fb} = -t_b \sum_{\langle i,j \rangle} f_j^\dagger f_i (b_i^\dagger + b_j) \quad (1)$$

mimics the correlations/fluctuations inherent to a spinful fermion many-particle system by a boson-affected transfer of spinless charge carriers. In Eq. (1), a fermion $f_i^{(\dagger)}$ creates (or absorbs) a local boson $b_i^{(\dagger)}$ every time it hops to a nearest-neighbor (NN) site j . Thereby it creates a local excitation in the background with energy ω_0 : $H_b = \omega_0 \sum_i b_i^\dagger b_i$. Because of quantum fluctuations, the background distortions should be able to relax with a certain rate λ . The entire Edwards

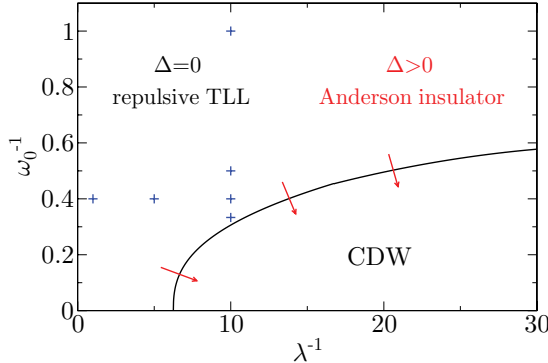


FIG. 1. (Color online) DMRG metal-insulator phase boundary for the 1D half-filled Edwards model without disorder (solid line). CDW order is suppressed if the background fluctuations dominate [$\omega_0 < 1$] or if the system's ability for relaxation is high [$\lambda > \lambda_c(\omega_0)$]. The blue crosses denote the parameter sets considered in this paper for the disordered Edwards model.

Hamiltonian then reads

$$H_E = H_{fb} - \lambda \sum_i (b_i^\dagger + b_i) + H_b. \quad (2)$$

A unitary transformation $b_i \mapsto b_i + \lambda/\omega_0$ eliminates the boson relaxation term in favor of a second fermion hopping channel:

$$H_E = H_{fb} - t_f \sum_{\langle i,j \rangle} f_j^\dagger f_i + H_b. \quad (3)$$

We like to emphasize that (i) this free-fermion transfer, however, takes place on a strongly reduced energy scale, $t_f = 2\lambda t_b/\omega_0$, and (ii) coherent propagation of a fermion is possible even in the limit $\lambda = t_f = 0$ by means of a six-step vacuum-restoring hopping process,²⁸ acting as a direct next-NN transfer “ $f_{i+2}^\dagger f_i$.” The Edwards model reveals a surprisingly rich physics. Depending on the relative strengths t_f/t_b of the two transport mechanisms and the rate of bosonic fluctuations t_b/ω_0 , it reproduces Holstein and t - J model-like lattice- and spin-polaron transport, respectively, in the single-particle sector.^{28,29} For the half-filled band case, a metal-insulator quantum phase transition from a repulsive Tomonaga-Luttinger-liquid (TLL) to a CDW has been reported,^{30,31} see Fig. 1. Note that the CDW is a few-boson state that typifies rather a correlated (Mott-Hubbard-type) insulator than a Peierls state with many bosons (phonons) involved.^{30,31} Since in the limit $\omega_0 \gg 1 \gg \lambda$ (here, and in what follows, t_b is taken as the unit of energy) background fluctuations are energetically costly, charge transport is hindered and an effective Hamiltonian with NN fermion repulsion results. To leading order, in a reduced (zero-boson) Hilbert space, we get

$$H_{tV} = -t_f \sum_{\langle i,j \rangle} f_j^\dagger f_i + V \sum_i n_i^f n_{i+1}^f, \quad (4)$$

with $V = t_b^2/\omega_0$. This so-called t - V model can be mapped onto the exactly solvable XXZ model, which exhibits a TLL-CDW quantum phase transition at $V/t_f = 2$, i.e., at $\lambda_c^{-1} = 4$. This value is smaller than those obtained for the Edwards model in the limit $\omega_0^{-1} \ll 1$, where $\lambda_c^{-1} \simeq 6.3$ (see Fig. 1 and Ref. 31),

because already three-site and effective next-NN hopping terms were neglected in the derivation of the t - V model.

We now employ the DMRG technique,²⁴ which can be easily generalized to treat systems including bosons,³² in order to obtain unbiased results for the full AEM,

$$H_{AE} = \Delta \sum_i \varepsilon_i n_i^f + H_E, \quad (5)$$

and the related At VM, $H_{AV} = \Delta \sum_i \varepsilon_i n_i^f + H_V$, where disorder of strength Δ is induced by independently distributed random on-site potentials ε_i , drawn from the box distribution $P(\varepsilon_i) = \theta(1/2 - |\varepsilon_i|)$. Within the pseudosite approach, a boson is mapped to n_b pseudosites.^{32,33} In the numerical study of the AEM, we take into account up to $n_b = 4$ pseudosites and determine n_b by the requirement that local boson density of the last pseudosite is less than 10^{-7} for all i . Furthermore, we keep up to $m = 1200$ density-matrix eigenstates in the renormalization steps to ensure that the discarded weight is smaller than 10^{-8} . The calculations are performed for finite systems with lengths $L = 16$ to 128 and open boundary conditions (OBC). For the simpler effective At VM, we reach $L = 192$ with OBC. Here the use of $m = 1000$ density-matrix eigenstates makes the discarded weight negligible. To gain representative results for our disordered systems, we proceed as follows. We first compute the physical quantity of interest at fixed L for numerous samples $\{\varepsilon_i\}$, then set up an appropriate statistical average, and finally perform a careful finite-size scaling.

III. FINITE-SIZE SCALING

An important question is, of course, which physical quantity to use in the finite-size scaling of the Anderson transition. For this purpose, the localization length ξ seems to be promising because it is sensitive to the nature, localized or extended, of the electron's eigenstate.^{34,35} So far, ξ has been determined from the phase sensitivity of the ground-state energy.^{17,25} Quite recently, Berkovits demonstrates that the entanglement entropy can also be used to extract the localization length.³⁶ However, in both methods, the system size L should be always larger than ξ .

Advantageously, the localization length can be extracted by a finite-size scaling analysis of the charge-density-structure factor even for $L \ll \xi$, which works equally well for interacting systems,²⁶ and therefore allows us to discuss the interplay between Anderson localization and CDW formation in a consistent manner. The charge structure is defined as

$$\tilde{C}(q) = \frac{1}{L} \sum_{i,r=1}^L [\langle n_i^f n_{i+r}^f \rangle - \langle n_i^f \rangle \langle n_{i+r}^f \rangle] e^{iqr}. \quad (6)$$

Assuming an exponential decay of the equal-time density-density correlations in the Anderson insulating phase,³⁷ the structure factor scales with

$$\tilde{C}(q) = -\frac{K_\rho^*}{2\pi^2} \frac{e^{-\frac{\pi^2 L}{6\xi}} - 1}{e^{\frac{\pi^2}{6\xi}} - 1} q^2, \quad (7)$$

where $q = 2\pi/L \ll 1$.²⁶ Equation (7) contains two unknown parameters: the localization length ξ and the disorder-modified

TLL interaction coefficient K_ρ^* . Hence, if the charge-structure factor is determined numerically, then ξ and K_ρ^* can be easily derived by fitting the numerical data with Eq. (7). For vanishing disorder, $\Delta \rightarrow 0$, ξ diverges and K_ρ^* becomes the ordinary TLL parameter K_ρ . We are aware that a disordered 1D system is no longer a TLL and, consequently, the TLL parameter is ill defined in the strict sense. Nevertheless, if the localization length significantly exceeds the lattice constant, then the short-range correlation functions should still show a power-law decay. Therefore, we might gain some valuable information about the local motion of fermions from K_ρ^* .

IV. DMRG RESULTS

Figure 2 demonstrates that the finite-size scaling of the averaged charge-structure factor $\tilde{C}_{av}(q)$ by means of (7) works best and equally well for the 1D AEM and At VM (this applies to all parameter values discussed below). To accommodate the missing correlations owing to the OBC, we have plotted $\tilde{C}_{av}(q)$ as a function of $1/(L - \delta)$ instead of $1/L$ (this way of plotting the data is nonessential but gives a quantitative refinement of the fit). The parameter δ is adjusted to reproduce $K_\rho^* = K_\rho$ and $\xi = \infty$ at $\Delta = 0$. We note the general tendency that the charge correlations arising at finite L will be suppressed as Δ becomes larger.

In a next step, we extract the localization length ξ and the modified TLL parameter for the disordered Edwards and t - V models. Figure 3 shows the dependence of ξ and K_ρ^* on the disorder strength Δ . First of all, we find a power-law decay of ξ with $1/\Delta$ in the whole ($\lambda, \omega_0; V$) parameter regime:

$$\xi/\xi_0 = \Delta^{-\gamma} \quad (8)$$

[note that Δ is given in units of t_b (t_f) in Fig. 3 for the AEM (At VM)]. The estimated values of the (bare) decay length ξ_0 and the exponent γ are given in the caption of Fig. 3 for characteristic model parameters. As expected, the localization length decreases with increasing disorder strength. Stronger electronic correlations, i.e., smaller λ or larger ω_0 (larger V) in the AEM (At VM), also tend to reduce ξ . In any case, ξ turns out to be finite as soon as $\Delta > 0$, indicating that

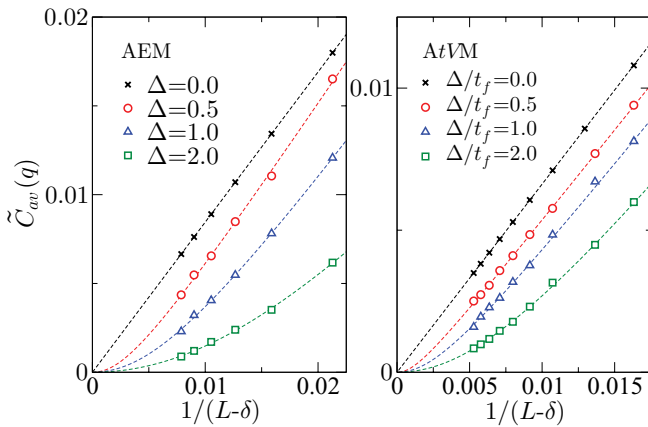


FIG. 2. (Color online) Charge-structure factor of the AEM with $\lambda = 0.1$ and $\omega_0 = 2$ (left panel) and the At VM with $V/t_f = 1.5$ (right panel) sampled over 300 and 500 disorder realizations, respectively. Dashed lines give the finite-size scaling of $\tilde{C}_{av}(q)$ according to (7).

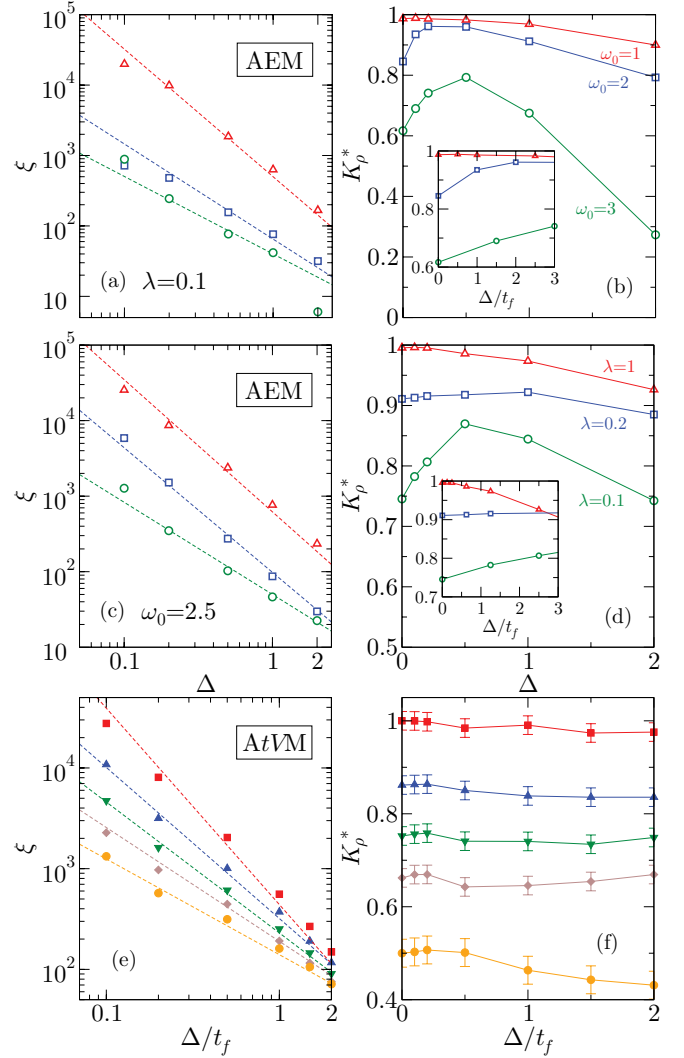


FIG. 3. (Color online) Left panels: Log-log plot of the localization length vs disorder strength for the AEM at (a) fixed $\lambda = 0.1$, (c) fixed $\omega_0 = 2.5$, and (e) for the At VM. Dashed lines are fits to Eq. (8) with (a) $\xi_0 = 620, 98, 50$ and $\gamma = 1.75, 1.65, 1.22$ for $\lambda = 1, 0.2, 0.1$; (c) $\xi_0 = 500, 65, 40$ and $\gamma = 1.81, 1.35, 1.1$ for $\omega_0 = 1, 2, 3$; and (e) $\xi_0 = 440, 350, 230, 190, 150$ and $\gamma = 1.95, 1.5, 1.3, 1.1, 0.95$ for $V/t_f = 0, 0.5, 1, 1.5, 2$ (from top to bottom), respectively. Right panels: Corresponding results for the modified TLL parameter K_ρ^* in the (b), (d) AEM and (f) At VM.

the repulsive TLL, if realized for $\Delta = 0$, makes way for an Anderson insulator. Thereby the localization length becomes comparable to the lattice spacing at $\Delta = 2$ in the AEM with $\lambda = 0.1, \omega_0 = 2.5$, while it is still about 10^2 for the At VM with $V/t_f = 2$.

The right-hand panels display striking differences in the Δ dependence of K_ρ^* for the models under consideration. These can be attributed to the fact that the Edwards model contains two energy scales λ and ω_0 , while the physics of the t - V model is merely governed by the ratio $V/t_f = t_b/2\lambda$, i.e., ω_0 drops out. Far away from the CDW instability, however, both models describe a weakly correlated TLL with $K_\rho \lesssim 1$, and K_ρ^* slowly decays as the disorder Δ increases (see the red open triangles in Fig. 3; to make the comparison with the t - V model data

easy, we have shown K_ρ^* versus Δ/t_f in the insets). If we move towards the CDW instability by decreasing λ at fixed $\omega_0 > \omega_{0,c}$ or increase ω_0 at $\lambda < \lambda_c$ (cf. Fig. 1), then a nonmonotonous behavior develops. At small Δ , K_ρ^* is significantly enhanced as the disorder increases. Obviously, weak disorder destabilizes the $2k_F$ -CDW correlations locally, since disorder-induced second- (and higher-) order boson-assisted (inelastic) hopping processes are possible in the AEM, even for $\omega_0 \gg 1$. This is in sharp contrast to the At VM, where only elastic scattering takes place and the intersite Coulomb repulsion is hardly affected by Δ . As a result, in the disordered t - V model, the CDW correlations will be stronger and more robust. Hence, for the At VM, K_ρ^* appears to be nearly independent from Δ for $0.5 \lesssim V/t_f \lesssim 2$. This also notably differs from the behavior found for the disordered Hubbard model,²⁶ where the umklapp scattering is effectively enhanced by the formation of Mott plateaus appearing due to disorder.³⁸ If Δ exceeds a certain value in the AEM, then K_ρ^* starts to decrease and, finally, the whole scaling procedure breaks down when $\xi \gtrsim 1$ (see the point at $\Delta = 2$ in the upper right panel with K_ρ^* well below 0.5). In this regime, the wave functions of the particles are strongly localized and the TLL behavior is as much suppressed as the CDW correlations. Let us point out that the enhancement of K_ρ^* triggered by the bosonic degrees of freedom might serve as an explanation for the observed increasing charge velocity near a negatively charged defect in the single-wall carbon nanotubes,¹¹ since the TLL parameter K_ρ is proportional to the charge velocity.

We now focus on the localization behavior at large distances [$O(\xi \gg 1)$], and therefore make an attempt to analyze the decay length ξ_0 and the exponent γ , for both the AEM and At VM, in terms of the interaction exponent K_ρ and the charge susceptibility χ_c of standard TLL theory.³⁷ We expect that ξ_0 is strongly influenced by the strength of the charge fluctuations quantified by χ_c , which is given—for the t - V model—as

$$\chi_c = \frac{2K_\rho}{\pi v_c} = \frac{4}{\pi \sqrt{1 - (\frac{V}{2t_f})^2}} \left[\frac{\pi}{\arccos(-\frac{V}{2t_f})} - 1 \right], \quad (9)$$

with charge velocity v_c . Figure 4 shows that ξ_0 nicely scales with V/t_f , i.e., $\xi_0 \propto \chi_c$, in fact (see upper panel). The same holds—perhaps surprisingly—for the AEM when ξ_0/t_f^γ is

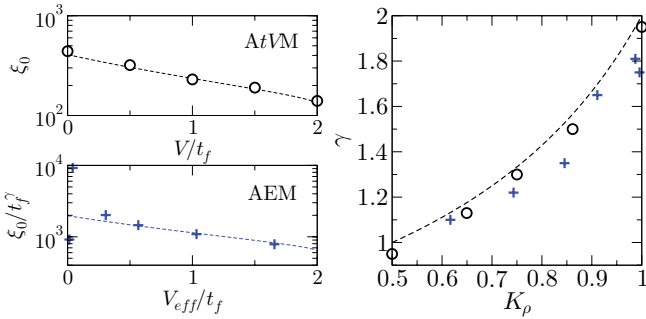


FIG. 4. (Color online) Left panels: Decay length ξ_0 as a function of the (effective) Coulomb repulsion V_{eff} for the At VM and AEM. Right panel: Corresponding γ exponent vs K_ρ , in comparison to the scaling relation (10) (dashed line). For further explanation, see text.

plotted versus an effective intersite repulsion estimated from $V_{\text{eff}}/t_f = -2 \cos(\pi/2K_\rho)$ (see lower panel). Moreover, for the disordered t - V model, the exponent γ is connected to K_ρ of the (spinless fermion) TLL system without disorder via the renormalization equation: $d(\Delta^2)/dl = (3 - 2K_\rho)\Delta^2$ (with scale quantity l). This causes the scaling relation^{37,39,40}

$$\gamma = 2/(3 - 2K_\rho). \quad (10)$$

The right panel of Fig. 4 displays that γ basically depends on K_ρ , as predicted by Eq. (10). This means that the long-range localization properties of the AEM can be understood in the framework of At VM with an effective intersite interaction induced by the bosonic degrees of freedom. Since the (effective) Coulomb repulsion tends to result in a lesser K_ρ , γ decreases with increasing V_{eff} (cf. Fig. 4). In this way, the $2k_F$ -CDW fluctuations triggered by V tend to weaken Anderson localization. While $\gamma = 2$ in the free-fermion limit ($V, 1/\lambda \rightarrow 0$), it scales to unity approaching the CDW transition point located, e.g., at $\lambda_c \simeq 0.07$ for $\omega_0 = 2.5$, respectively, at $\omega_{0,c} \simeq 3.1$ for $\lambda = 0.1$.

The question of how disorder affects the insulating CDW state could not be addressed by the above TLL-based scaling. In particular, we cannot assess by our numerical approach whether the CDW phase survives *weak* disorder (as experimentally observed for disordered Peierls-Mott insulators).¹⁰ If the Imry-Ma argument for disordered (low-D) interacting systems⁴¹ holds, then CDW long-range order should be destroyed by any finite Δ . Figure 5, showing the spatial variation of the local fermion/boson densities for a specific but typical disorder realization (note that any real experiment is performed on a particular sample), illustrates the situation deep inside the (former) CDW phase ($\lambda^{-1} = 100$, $\omega_0^{-1} = 0.4$; cf. Fig. 1). One realizes that long-range charge order ceases to exist but short-range CDW correlations locally persist whenever neighboring on-site potentials do not differ much (see, e.g., the region $i = 45, \dots, 55$ in the lower panel of Fig. 5).

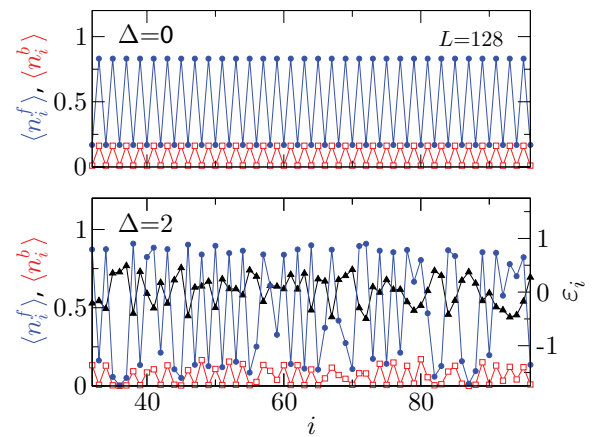


FIG. 5. (Color online) Local densities of fermions $\langle f_i^\dagger f_i \rangle$ (blue circles) and bosons $\langle b_i^\dagger b_i \rangle$ (red open squares) in the central part of an open AEM chain without ($\Delta = 0$) and with ($\Delta = 2$) disorder. Results are given for a single realization $\{\varepsilon_i\}$ (black triangles). Model parameters are $\lambda = 0.01$, $\omega_0 = 2.5$, and $L = 128$ (OBC).

V. CONCLUSIONS

To summarize, using an unbiased numerical DMRG approach, we investigated the interplay of disorder and interaction effects including bosonic degrees of freedom in the framework of the 1D spinless fermion Anderson-Edwards model. Although the TLL phase disappears owing to the disorder, the localization properties of the Anderson insulator state can be understood in terms of scaling relations containing the charge susceptibility and the Luttinger liquid parameter of the metallic phase without disorder only, as in the case of the spinless fermion Anderson- t - V model. However, the

Anderson-Edwards model reveals a more complex interrelation between disorder and CDW correlations because additional scattering channels, involving bosonic excitation and annihilation processes, appear. This offers a promising route for adapting the description of low-dimensional transport in many disordered materials. Disorder also affects the CDW state in that true long-range order vanishes although local CDW correlations survive.

ACKNOWLEDGMENT

This work was supported by DFG through SFB 652.

-
- ¹V. F. Gantmakker, in *Electrons And Disorder in Solids*, International Series of Monographs on Physics Vol. 130 (Clarendon, Oxford, 2005).
- ²P. W. Anderson, *Phys. Rev.* **109**, 1492 (1958).
- ³J. Fröhlich, F. Martinelli, E. Scoppola, and T. Spencer, *Commun. Math. Phys.* **101**, 21 (1985).
- ⁴N. F. Mott, *Metal-Insulator Transitions* (Taylor & Francis, London, 1990).
- ⁵L. D. Landau, *Phys. Z. Sowjetunion* **3**, 664 (1933).
- ⁶R. Peierls, *Quantum Theory of Solids* (Oxford University Press, Oxford, 1955).
- ⁷N. Tsuda, K. Nasu, A. Yanase, and K. Siratori, *Electronic Conduction in Oxides* (Springer-Verlag, Berlin, 1991).
- ⁸A. R. Bishop and B. I. Swanson, *Los Alamos Sci.* **21**, 133 (1993).
- ⁹D. Jérôme and H. J. Schulz, *Adv. Phys.* **31**, 299 (1982).
- ¹⁰C. Weber, D. D. O'Regan, N. D. M. Hine, M. C. Payne, G. Kotliar, and P. B. Littlewood, *Phys. Rev. Lett.* **108**, 256402 (2012).
- ¹¹I. O. Maciel, N. Anderson, M. A. Pimenta, A. Hartschuh, H. Qian, M. Terrones, H. Terrones, J. Campos-Delgado, A. M. Rao, L. Novotny *et al.*, *Nature Mater.* **7**, 878 (2008).
- ¹²S. Ciuchi and S. Fratini, *Phys. Rev. Lett.* **106**, 166403 (2011).
- ¹³Z. Ristivojević, A. Petković, P. Le Doussal, and T. Giamarchi, *Phys. Rev. Lett.* **109**, 026402 (2012).
- ¹⁴E. Abrahams, *50 Years of Anderson Localization* (World Scientific, Singapore, 2010).
- ¹⁵P. W. Anderson, *Nature (London)* **235**, 163 (1972).
- ¹⁶F. X. Bronold and H. Fehske, *Phys. Rev. B* **66**, 073102 (2002).
- ¹⁷H. Ebrahimnejad and M. Berciu, *Phys. Rev. B* **85**, 165117 (2012).
- ¹⁸M. A. Tusch and D. E. Logan, *Phys. Rev. B* **48**, 14843 (1993).
- ¹⁹V. Dobrosavljević and G. Kotliar, *Phys. Rev. Lett.* **78**, 3943 (1997).
- ²⁰K. Byczuk, W. Hofstetter, and D. Vollhardt, *Phys. Rev. Lett.* **94**, 056404 (2005).
- ²¹A. Farhoodfar, R. J. Gooding, and W. A. Atkinson, *Phys. Rev. B* **84**, 205125 (2011).
- ²²D. Tanasković, V. Dobrosavljević, E. Abrahams, and G. Kotliar, *Phys. Rev. Lett.* **91**, 066603 (2003).
- ²³S. Chiesa, P. B. Chakraborty, W. E. Pickett, and R. T. Scalettar, *Phys. Rev. Lett.* **101**, 086401 (2008).
- ²⁴S. R. White, *Phys. Rev. Lett.* **69**, 2863 (1992).
- ²⁵P. Schmitteckert, T. Schulze, C. Schuster, P. Schwab, and U. Eckern, *Phys. Rev. Lett.* **80**, 560 (1998).
- ²⁶S. Nishimoto and T. Shirakawa, *Phys. Rev. B* **81**, 113105 (2010).
- ²⁷D. M. Edwards, *Physica B* **378–380**, 133 (2006).
- ²⁸A. Alvermann, D. M. Edwards, and H. Fehske, *Phys. Rev. Lett.* **98**, 056602 (2007).
- ²⁹M. Berciu and H. Fehske, *Phys. Rev. B* **82**, 085116 (2010).
- ³⁰G. Wellein, H. Fehske, A. Alvermann, and D. M. Edwards, *Phys. Rev. Lett.* **101**, 136402 (2008).
- ³¹S. Ejima, G. Hager, and H. Fehske, *Phys. Rev. Lett.* **102**, 106404 (2009).
- ³²E. Jeckelmann and S. R. White, *Phys. Rev. B* **57**, 6376 (1998).
- ³³E. Jeckelmann and H. Fehske, *Riv. Nuovo Cimento* **30**, 259 (2007).
- ³⁴E. Abrahams, P. W. Anderson, D. C. Licciardello, and T. V. Ramakrishnan, *Phys. Rev. Lett.* **42**, 673 (1979).
- ³⁵B. Kramer and A. Mac Kinnon, *Rep. Prog. Phys.* **56**, 1469 (1993).
- ³⁶R. Berkovits, *Phys. Rev. Lett.* **108**, 176803 (2012).
- ³⁷T. Giamarchi and H. J. Schulz, *Phys. Rev. B* **37**, 325 (1988).
- ³⁸M. Okumura, S. Yamada, N. Taniguchi, and M. Machida, *Phys. Rev. Lett.* **101**, 016407 (2008).
- ³⁹F. Woynarovich and H. P. Eckle, *J. Phys. A* **20**, L97 (1987).
- ⁴⁰C. J. Hamer, C. R. W. Quispel, and M. T. Batchelor, *J. Phys. A* **20**, 5677 (1987).
- ⁴¹Y. Imry and S. Ma, *Phys. Rev. Lett.* **35**, 1399 (1975).